

Project 2- A Discontinuous Galerkin (Finite Volume) program for solving the Compressible Euler Equations

Sujal Dave (200254193)

Abstract

Partial differential equations play an important role in engineering applications. It is often possible to solve these equations only approximately, i.e. numerically. Therefore, number of successful discretization techniques has been developed to solve these equations. The Discontinuous Galerkin method seems to be very general method to solve this type of equations, especially useful for hyperbolic systems. The aim in this project is to solve the 2-D Euler equations around a number of test objects like a NACA 0012 airfoil, Cylinder and a Channel flow with a bump. This system of equations is indeed hyperbolic and therefore the discontinuous Galerkin method was chosen. The most important aspect of this method is its ability to deal with complex geometries, possibility of high-order method and its local character enabling efficient computation parallelization.

Keywords: CFD, Discontinuous Galerkin, Finite Volume, Euler Equations

1. Introduction

The central theme of this project is to solve the classical fluid phenomena using the most general Euler equations. Since it is a very difficult to undertake the experiments for a number of fluid flow phenomena like an aircraft flying high in the atmosphere, or a supersonic or hypersonic flow condition for any geometry. The development of a wind tunnel has necessitated a lot of research in the fluids field but yet the high cost of the project is almost impossible to reduce. Hence, the field of computational fluid dynamics (CFD) has emerged in the recent time because of the advent of high computing processors and increased accuracy of the results. The power of today computers makes it even possible to solve directly the most general Navier-Stokes equations (NSEs) governing fluid dynamics. These methods involve Direct Numerical Simulation (DNS), Large Eddy Simulation (LES), Reynolds Averaged Numerical Simulation (RANS) etc. We have a broad choice of commercial software for Computational Fluid Dynamics (CFD) simulations, e.g. ANSYS CFX, ANSYS Fluent, COMSOL Multiphysics or Star-CCM+, as well as some successful open-source/freeware alternatives like OpenFOAM.

Email address: `sdcv@ncsu.edu` (Sujal Dave (200254193))

2. Problem Description and Solution Methodology

2.1. Hyperbolic Equations

Consider a second order PDE written in the form as shown in the equation below

$$Au_{xx} + Bu_{xy} + Cu_{yy} + Du_x + Eu_y + F = G \quad (1)$$

$$B^2 - 4AC > 0 \quad (2)$$

If, this equation satisfies the condition in equation (2), then the equation is known as a Hyperbolic Equation.

A classical example of a hyperbolic equation is a wave equation. The Euler equations that will be solved numerically in this project, fall under the hyperbolic partial differential equations category.

2.2. Euler Equations

The Navier-Stokes equations that were derived for incompressible flows may be applied for any Newtonian fluid whether it is viscous or inviscid. Since real fluids are viscous, it may seem useless to study inviscid flows. However, to understand the real behavior of fluid flows, the study of inviscid flows becomes extremely important. There are certain viscous flows, which behave like an inviscid flow for all practical purposes. For example, flows outside the viscous boundary layer fall into this category. Even today, most of the aerodynamic analysis is based upon ideal flow theory.

By substituting the viscous terms to be zero in the Navier-Stokes equation, we arrive at the Euler Equations as shown below,

$$\partial u / \partial x + \partial v / \partial y = 0 \quad (3)$$

$$u \partial u / \partial x + v \partial u / \partial y = -1/\rho \partial p / \partial x \quad (4)$$

$$u \partial v / \partial x + v \partial v / \partial y = -1/\rho \partial p / \partial y \quad (5)$$

Hence, we have, three variables (u,v and p) in 2-D and the corresponding 3 equations in order to solve the system.

It is easier to write the Euler equations in a conservative form which reads,

$$\partial \mathbf{U} / \partial t + \partial \mathbf{F} / \partial x + \partial \mathbf{G} / \partial y = 0 \quad (6)$$

where

$$\mathbf{U} = \begin{bmatrix} \rho \\ \rho u \\ \rho v \\ \rho E \end{bmatrix} \quad \mathbf{F} = \begin{bmatrix} \rho u \\ \rho u^2 + p \\ \rho uv \\ u(\rho E + p) \end{bmatrix} \quad \mathbf{G} = \begin{bmatrix} \rho v \\ \rho uv \\ \rho v^2 + p \\ v(\rho E + p) \end{bmatrix} \quad (7)$$

here, $p = (\gamma - 1)(E - \rho(u^2 + v^2)/2)$

2.3. Discontinuous Galerkin Method

The discontinuous Galerkin method is a class of finite element methods using completely discontinuous piecewise polynomial space for the numerical solution and the test functions. One certainly needs to use more degrees of freedom because of the discontinuities at the element boundaries, however this also gives one a room to design suitable inner boundary treatments (fluxes) to obtain highly accurate and stable methods in many difficult situations.

The discontinuous Galerkin method has found rapid applications in a number of diverse application like the aerospace industry and general fluid flow problem applicable widely in industry.

The discontinuous Galerkin method has a number of advantages

- It can be designed for any order of accuracy in space and time.
- It can easily adapt to changes since the refinement of the mesh can be achieved without taking in account the continuity restrictions
- No global linear or non-linear system needs to be solved
- Good Stability and highly compact

2.4. Solution Methodology

The solution of the Euler equations is highly dependent on the initial Mach number that we provide in the domain. The various fluxing schemes that incorporate the Flux vector splitting methods are based on the local Mach numbers in the flow. The van-Leer Flux vector splitting method is used in this project which gives the flux at the positive and negative side of the face as follows,

$$F_{VLS}^{\pm} = \begin{pmatrix} f_1^{\pm} \\ f_1^{\pm} \frac{(\gamma - 1)u \pm 2c}{\gamma} \\ f_1^{\pm} \frac{((\gamma - 1)u \pm 2c)^2}{2(\gamma^2 - 1)} \end{pmatrix} \quad (8)$$

In order to create the second order solution from the Finite Volume method, the MUSCL slope limiter approach [1] is used which reconstructs the slope according to the underlying formula,

$$\begin{aligned} u_{i+1/2}^L &= u_i + \frac{\varphi(r_i)}{4} [(1-k)\partial u_{i-1/2} + (1+k)\partial u_{i+1/2}] \\ u_{i+1/2}^R &= u_{i+1} + \frac{\varphi(r_{i+1})}{4} [(1-k)\partial u_{i+3/2} + (1+k)\partial u_{i+1/2}] \end{aligned} \quad (9)$$

The approach used for the unstructured grids is the van-Albada limiter,

$$\varphi_{val}(r) = \frac{r^2 + r}{r^2 + 1} \quad (10)$$

While solving the MUSCL approach, we see that we have more number of equations than the number of unknowns. Hence we use the least squares reconstruction method in order to calculate the gradients of the flow variables.

The equations are advanced in time used the TVD RK-3 schemes. [2]

The boundary conditions used for the Airfoil and Cylinder geometry is the Solid Wall and Far Field boundary condition whereas addition conditions of Subsonic In/Outflow and Supersonic In/Outflow had to be defined in order to capture the high mach number flow in that case.

The error in the case is calculated from the entropy in the problem. For the entropy S , pressure p , density ρ and Heat capacity ratio γ

$$S = \frac{p}{\rho^\gamma}$$

The, for NELEM being the number of elements in the domain, the error is given by

$$Error = \sqrt{\frac{(\frac{S_\infty - S}{S_\infty})^2}{NELEM}}$$

3. Results

3.1. Subsonic Flow Past a circular cylinder

Test case conditions :

1. Mach number = 0.38
2. Slip Wall conditions at cylinder wall
3. Boundaries are given the Far field conditions
4. Mesh files considered - Coarse, Medium, Fine, Very Fine

3.1.1. Mesh files for the circular cylinder

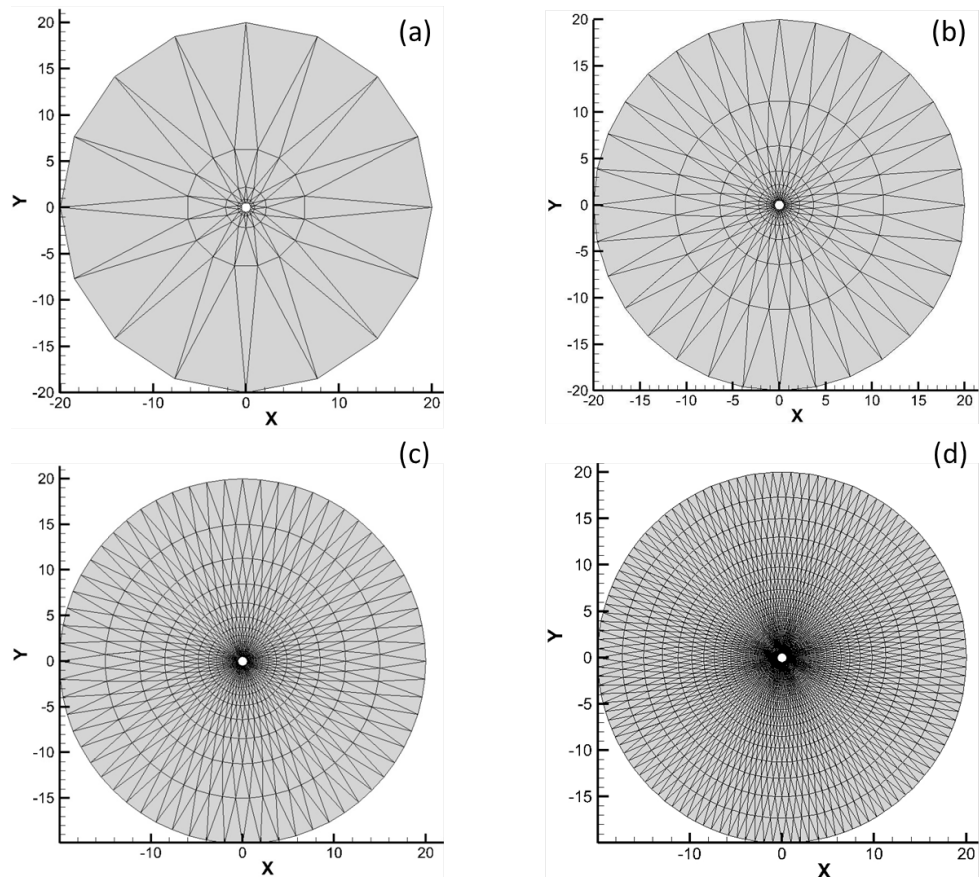


Figure 1: Different type of meshes in order to run Subsonic cases ($M=0.38$). As we go from (a) to (d) we can see a finer grid.

3.1.2. Contours of Pressure, Density and Mach Number and Residual Plots

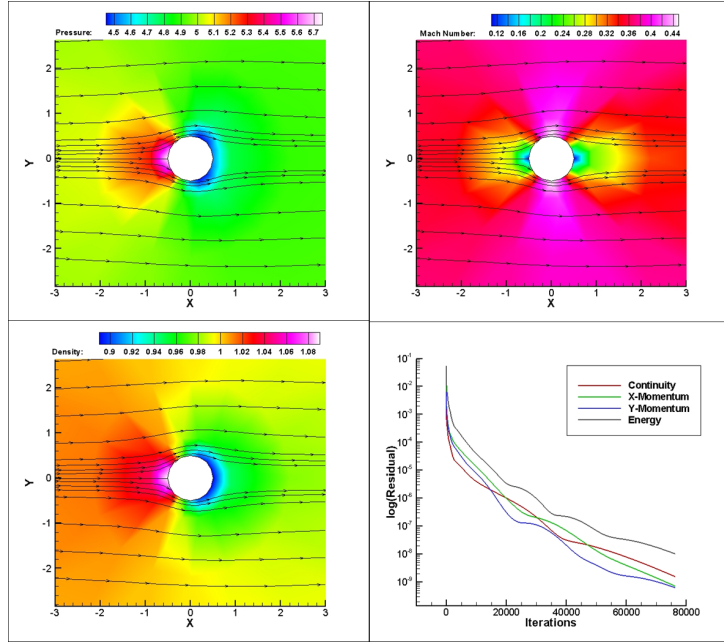


Figure 2: Pressure, Mach Number and Density Contours for a Coarse mesh. The residual plot is adjoining.

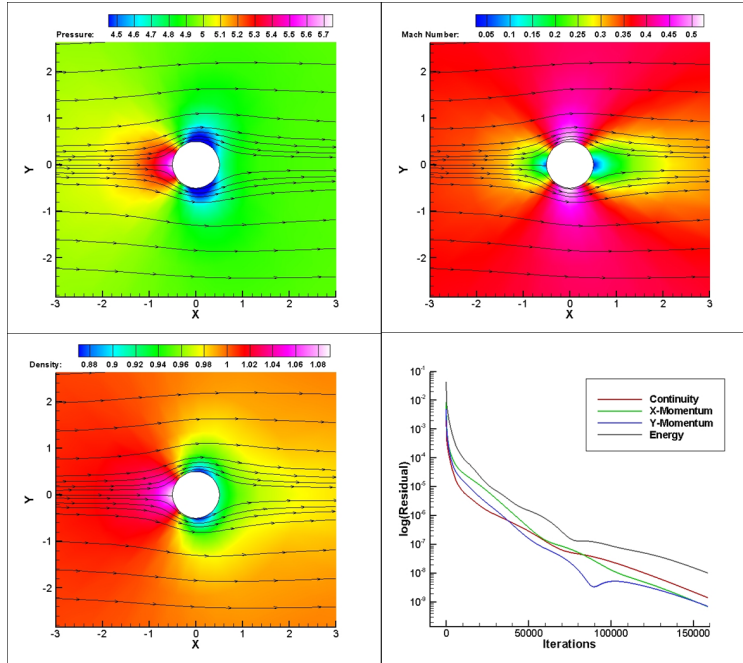


Figure 3: Pressure, Mach Number and Density Contours for a Medium mesh. The residual plot is adjoining.

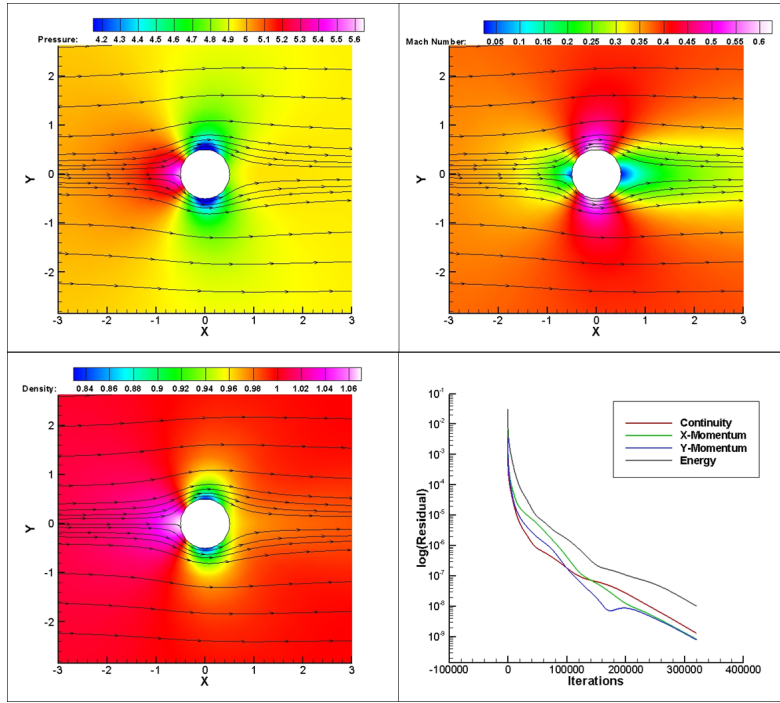


Figure 4: Pressure, Mach Number and Density Contours for a Fine mesh. The residual plot is adjoining.

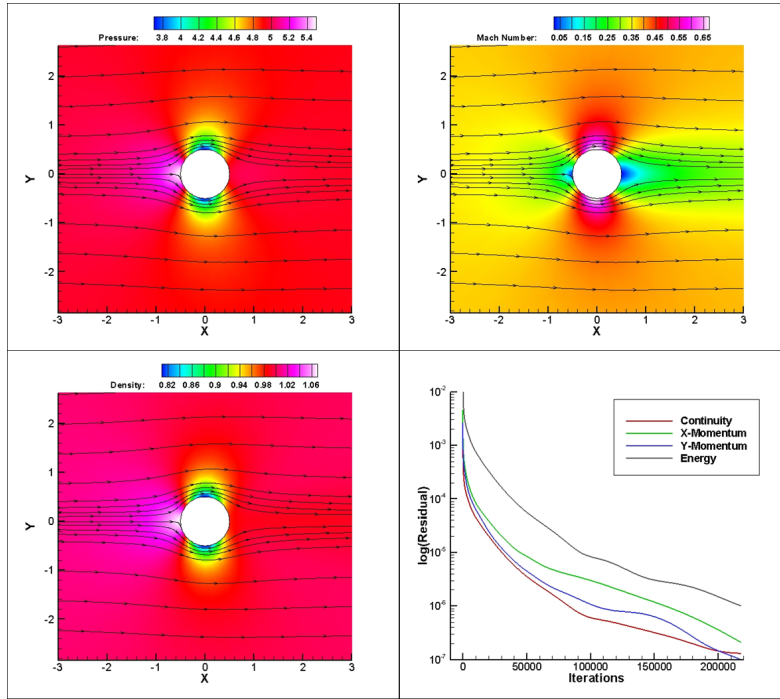


Figure 5: Pressure, Mach Number and Density Contours for a Very Fine mesh. The residual plot is adjoining.

3.1.3. Grid Convergence Study

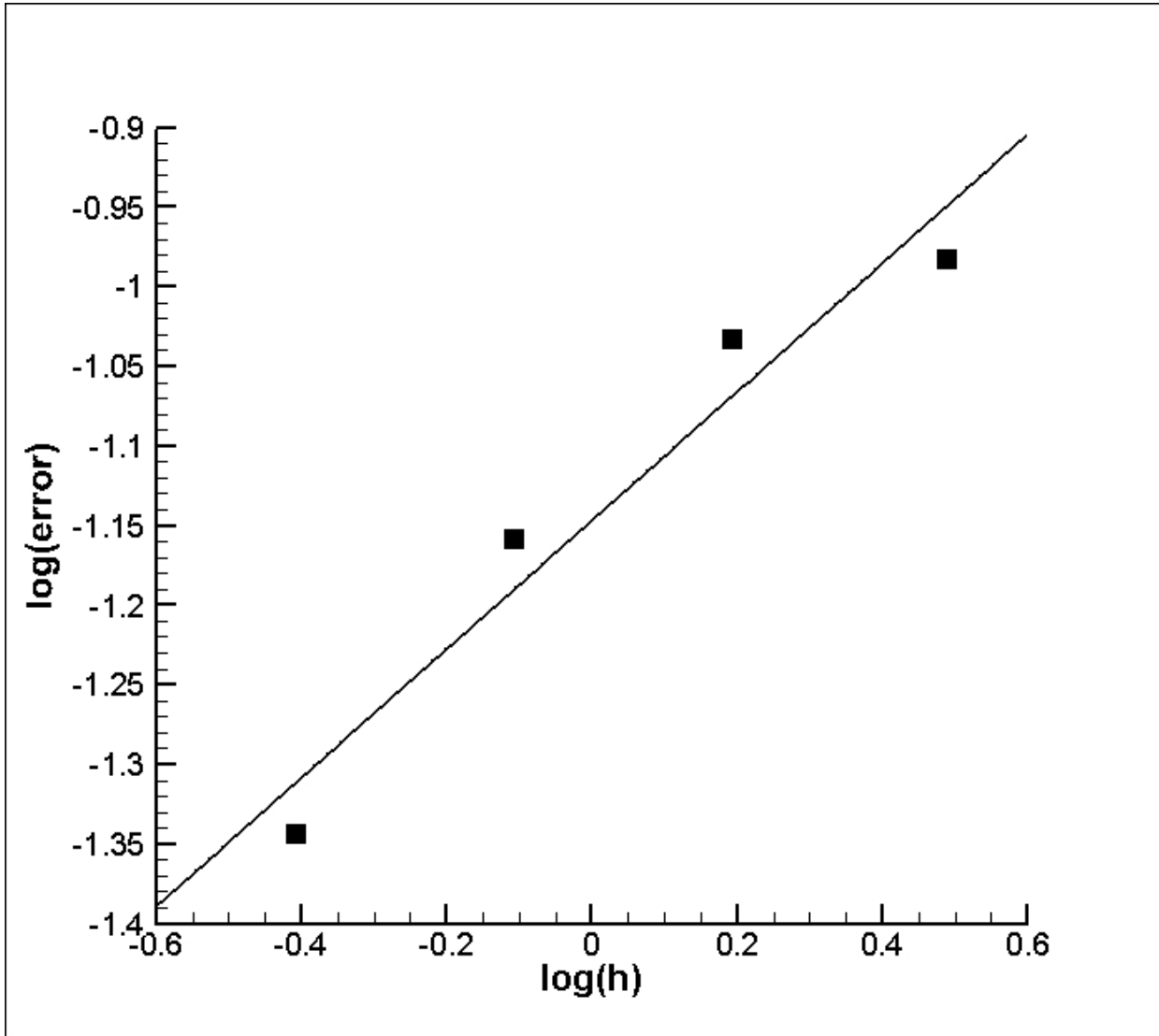


Figure 6: Grid convergence study of the various meshes analysed.

3.1.4. Observations

- The contours for the subsonic Mach number of 0.38 shows the solution to be relatively smooth over the domain without any discontinuities or shock.
- The residual plots are used to monitor the solution and they give the information about the solution at different time steps. The residual for continuity converges the fastest.
- The grid convergence study tells us that as we increase the grid size, the error increases.

3.2. Transonic flow past a NACA 0012 airfoil

Test case conditions :

1. Mach number = 0.85
2. Angle of attack = 1 degree.
3. Slip Wall conditions airfoil walls
4. Boundaries are given the Far field boundary conditions

3.2.1. Mesh files for NACA airfoil

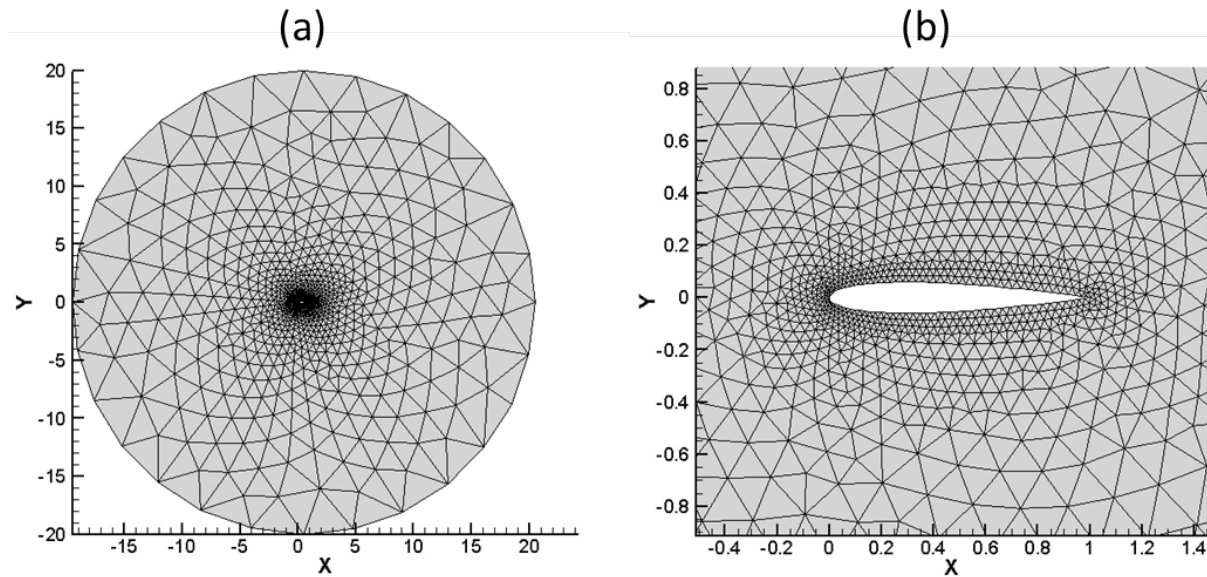


Figure 7: Mesh taken into consider to analyse the transonic floww ($M=0.85$). (Right) is the zoomed in view of the airfoil NACA 0012

3.2.2. Contours of Pressure, Density and Mach Number and Residual Plots

Figure 8 shows the the contour plots and the residual plots

3.2.3. Observations

- In transonic flow over the NACA 0012 airfoil we see the formation of a shock downstream of the leading edge of airfoil.
- The initially subsonic flow expands as it goes over the airfoil reaches a supersonic flow and then encounters a shock wave.
- A higher pressure is observed at the bottom surface than at the top surface which tells us that the net force on the airfoil is upwards.
- This shows that a 1 angle of attack, gives a lift to the airfoil.
- The change in Mach no. across the shock wave is from approximately 0.8 to 1.2.

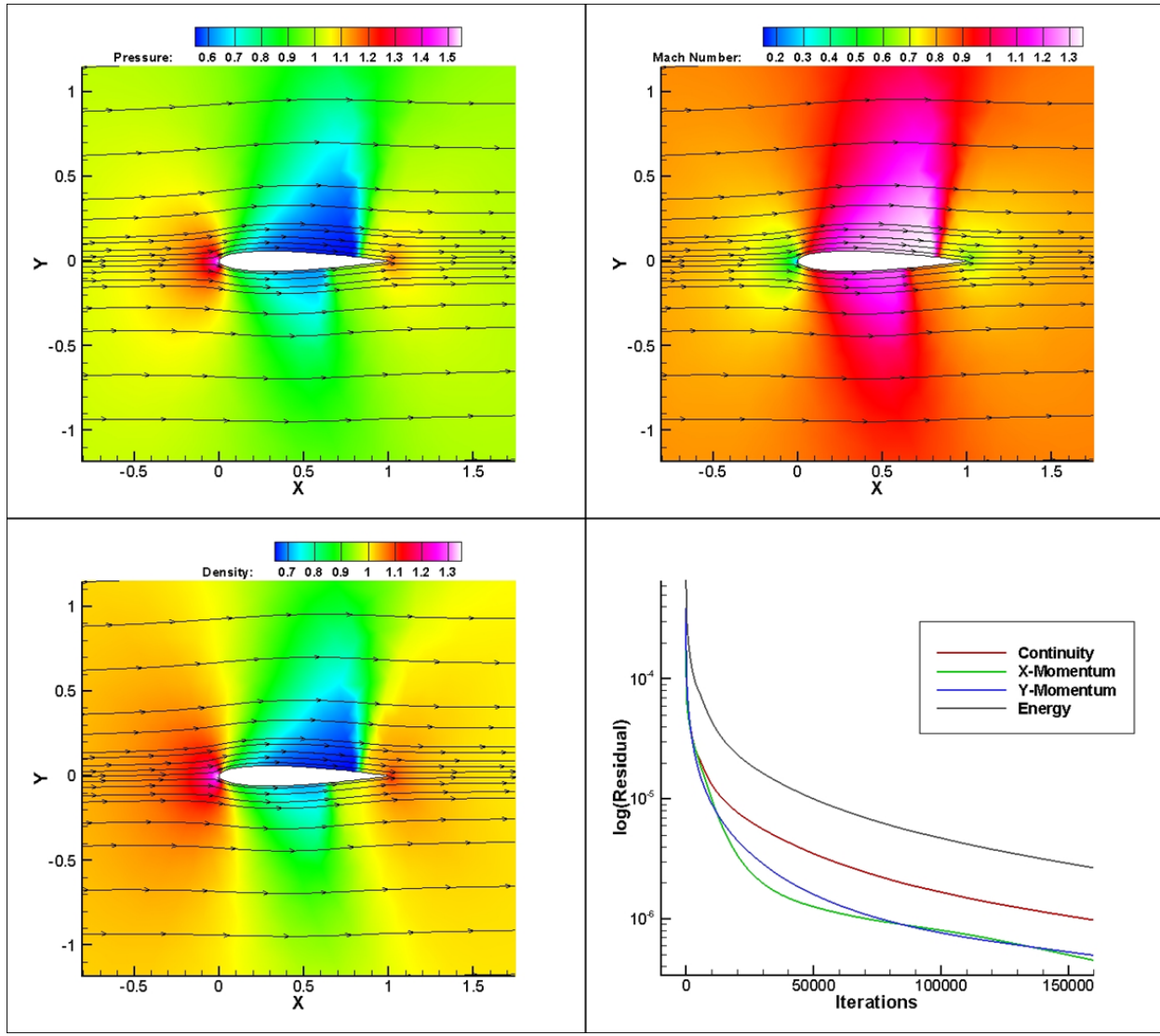


Figure 8: Pressure, Mach Number and Density Contours for the airfoil. The residual plot is adjoining.

3.3. Supersonic flow in a channel with bump

Test case conditions :

1. Mach number = 1.1
2. Slip Wall conditions at the top and bottom walls
3. Left and right boundaries are defined using the Subsonic/Supersonic inflow and outflow conditions.

3.3.1. Mesh file for the Channel with bump

3.3.2. Contours of Pressure, Density and Mach Number and Residual Plots

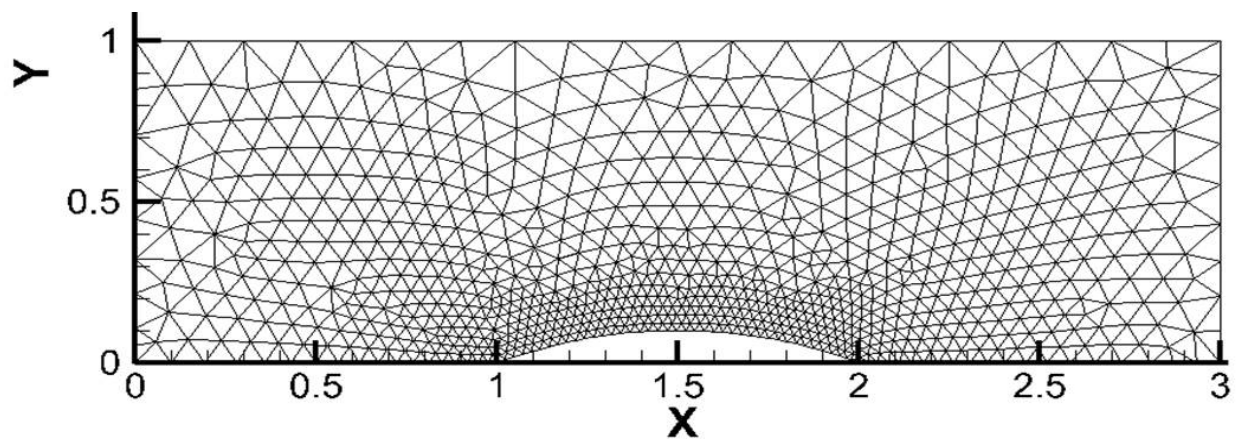
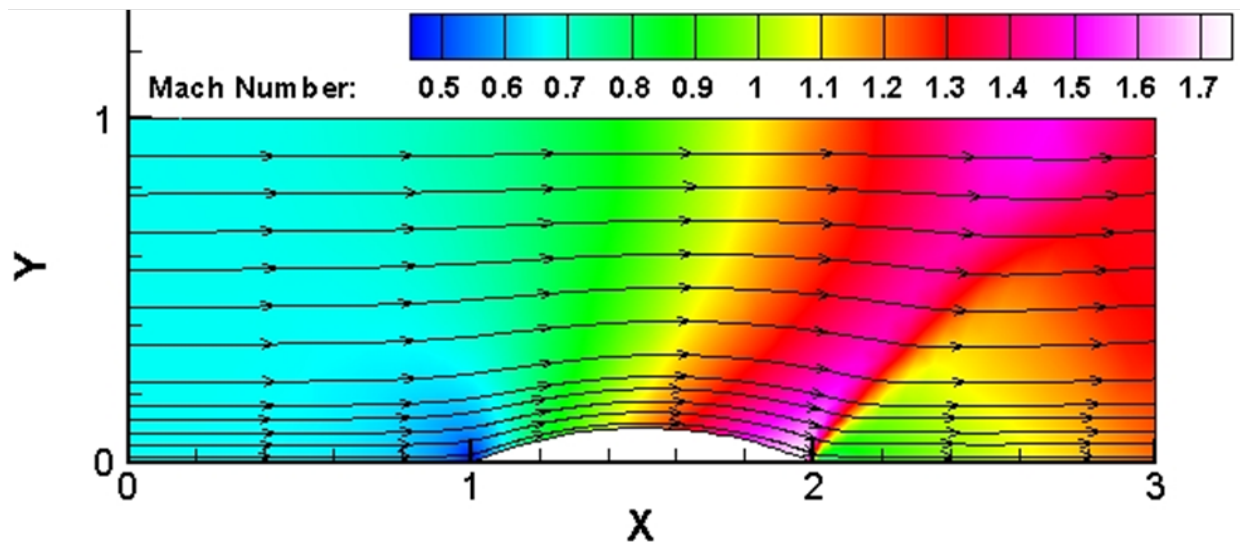
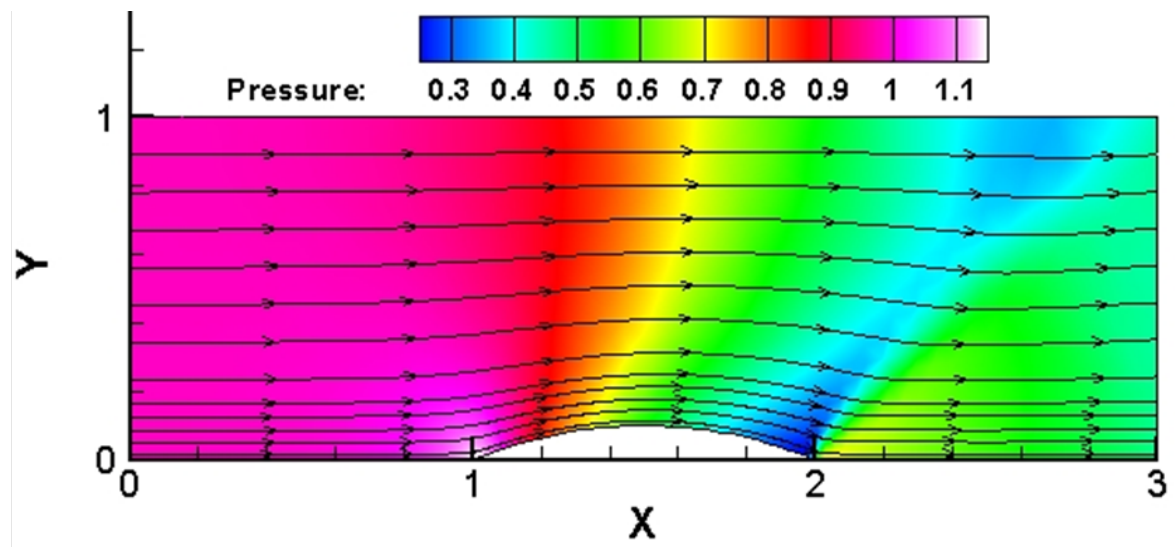


Figure 9: Mesh file of the channel with bump case for transonic flow ($M=1.1$)



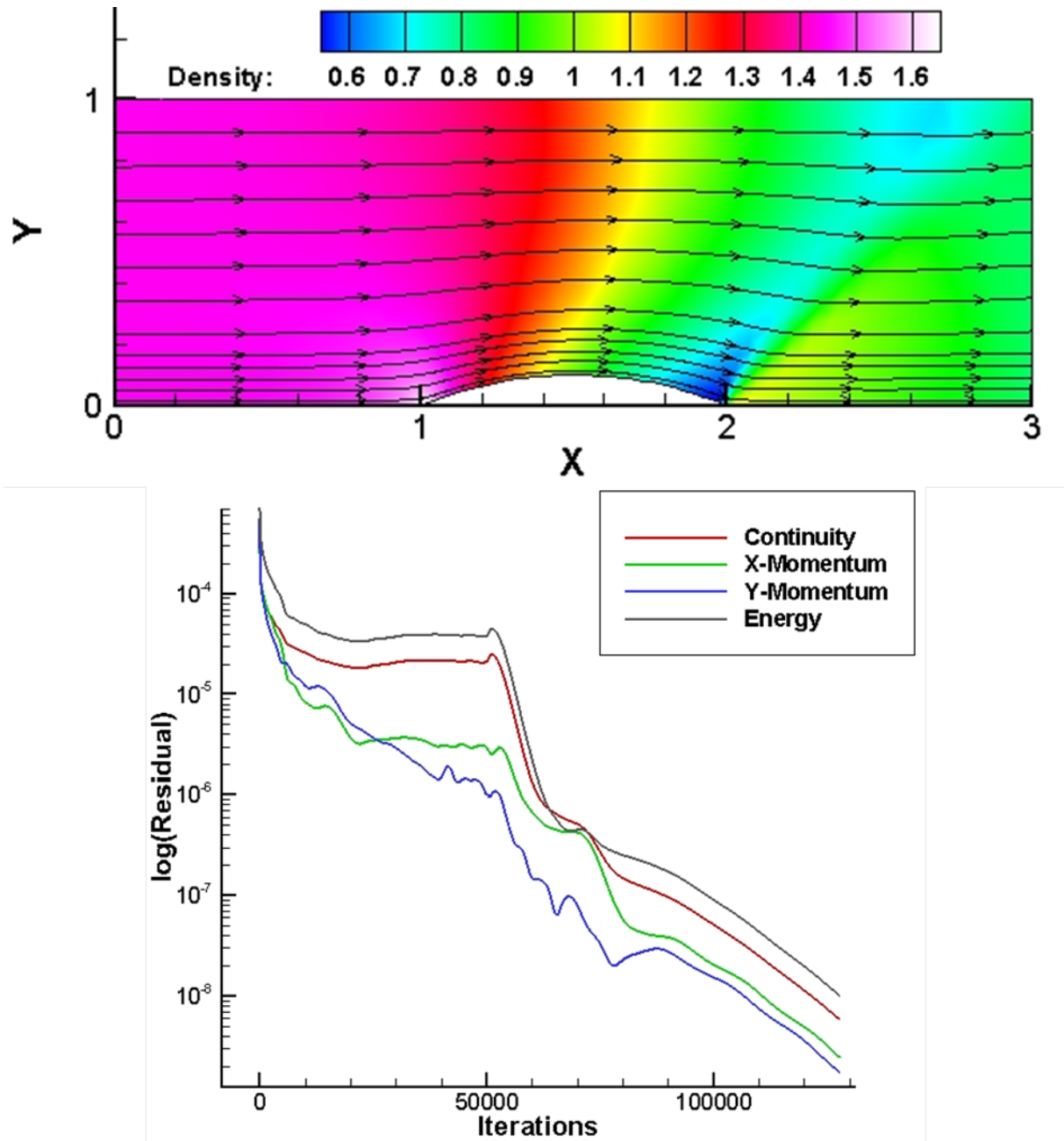


Figure 10: Pressure, Mach Number and Density Contours for the airfoil and the residual plot.

3.3.3. Observations

- Initially transonic conditions at the inlet, the flow moves towards the bump and decelerates over the bump where the sonic conditions are reached which result in a choke flow.

- The shock can be seen as stronger towards the top and bottom walls rather than the centre region of the flow.

4. Conclusion

A finite volume DG solver using the Van-Leer flux splitting method was tested on three different geometries with different flow conditions and boundary conditions. The grid convergence study for the cylinder subsonic flow case was conducted and it was established that upon reducing the grid size, the error also reduces. The transonic flow past NACA 0012 airfoil at 1° angle of attack showed a shock formation downstream and also depicted a positive lift force on the airfoil. Supersonic channel flow with a bump showed the shock formed in the channel.

References

- [1] C. Laney, Computational Gasdynamics, Cambridge University Press, Cambridge, 1998.
- [2] Total variation diminishing Runge-Kutta schemes, Sigal Gottlieb and Chi-Wang Shu, *Math. Comp.* 67 (1998) 73–85.